

DOI: 10.1002/adma.200801024

Vacuum-Processed Polyaniline–C₆₀ Organic Field Effect Transistors**

By Mihai Irimia-Vladu,* Nenad Marjanovic, Angela Vlad, Alberto Montaigne Ramil, Gerardo Hernandez-Sosa, Reinhard Schwödianer, Siegfried Bauer and Niyazi Serdar Sariciftci

The transfer of laboratory knowledge into large-scale industrial production processes represents a great challenge in the field of organic electronics. Potential applications of organic electronics may arise in low-cost, large-area flexible devices such as voltage inverters, sensors, smart cards, nonvolatile memories, flexible display driver circuits, frequency information tags, that is, inventory labels and price tags, and others. Today the performance of the best organic field effect transistors (OFETs)^[1,2] rivals that of commercial amorphous hydrogenated silicon transistors, currently employed as the pixel switching element in active-matrix flat-panel displays. Large-scale industrial production of organic electronics is envisioned as roll-to-roll (R2R) processing. Nowadays avenues toward R2R processes comprise various solution-based large-area printing steps. On the other hand, vacuum-based thermal evaporation R2R processes are often used in metallization of polymer foils for food packaging. Here we report on the processing of OFETs by thermal evaporation of organic gate dielectrics and semiconductors. Organic–organic interfaces between the dielectric and semiconductor

may result in lower charge trap densities in comparison to organic–inorganic interfaces.^[3] For the active semiconductor we have chosen C₆₀, while polyaniline is employed as organic gate dielectric. Our results also suggest processing of an OFET solely made of evaporated polyaniline, because polyaniline can efficiently work as conductor, insulator, and semiconductor.^[4,5] Using R2R thermal evaporation as a technology for mass production of organic electronics based on dielectrics and small-molecule active materials could be an alternative for the solution-processing large-area printing. Ultimately, combining these two technologies in a hybrid approach might be the strategy for versatile mass production of organic electronics.

Polyaniline is known as the first polymer ever synthesized; the first report of aniline black dates back nearly two centuries ago.^[6] The interest in polyaniline rose tremendously nearly two decades ago,^[7–12] following the discovery of conducting polymers by MacDiarmid, Shirakawa, and Heeger. Today polyaniline remains one of the most investigated conductive polymers, owing to its ease of synthesis and processibility in organic solvents, low synthetic cost, excellent shelf-life stability, and easy conversion between insulating, semiconducting, and conducting states by simple chemical reactions.^[5,13–19] A schematic of polyaniline in various oxidation states is displayed in Figure 1. Water-soluble functionalized polyaniline has found its applicability in various organic electronic devices; as organic semiconductor in light emitting diodes,^[20–22] in conductive form as an alternative to metallic electrodes in organic electronics,^[23,24] and as a semiconducting layer in OFETs.^[25,26]

Solution casting is not the only way polyaniline can be processed. Polyaniline in the emeraldine oxidation state can also be deposited onto solid substrates by vapor deposition. One of the first reports dealing with evaporated polyaniline appeared two decades ago^[10] and the chemical and electronic properties of the thin polyaniline films as well as their interface with metal electrodes was intensely studied by various groups over the past decade.^[27–31] In this work, we show the applicability of polyaniline as an insulating gate layer in OFETs. We used no solution processing in the fabrication process of the field effect transistor; instead both polyaniline and the small molecule semiconductor (i.e., C₆₀) layers are successively evaporated without breaking the vacuum in the evaporation chamber.

A scheme of the transistor structure is shown in Figure 2. The transistor is evaporated on glass substrates in a vacuum

[*] Dr. M. Irimia-Vladu, Dr. R. Schwödianer, Prof. S. Bauer
Department of Soft Matter Physics
Johannes Kepler University
Altenberger Strasse Nr. 69, 4040 Linz (Austria)
E-mail: mihai.irimia-vladu@jku.at

Dr. N. Marjanovic, Dr. A. Montaigne Ramil
plastic electronic GmbH
Rappetsederweg Nr. 28, 4040 Linz (Austria)

A. Vlad
Institute of Applied Physics
Johannes Kepler University
Altenberger Strasse Nr. 69, 4040 Linz (Austria)

G. Hernandez-Sosa
Institute of Semiconductor and Solid State Physics
Johannes Kepler University
Altenberger Strasse Nr. 69, 4040 Linz (Austria)

Prof. N. S. Sariciftci
Linz Institute for Organic Solar Cells (LIOS), Physical Chemistry
Johannes Kepler University Linz
Altenberger Strasse Nr. 69, 4040 Linz (Austria)

[**] The authors thank Dr. Birendra Singh, Dr. Yohannes Teketel, Dr. Pavel Troshin, Dr. Serap Günes, and Phillipp Stadler, for fruitful discussions and/or suggestions during experimental design. Thanks are also conveyed to Prof. Bäuerle (Institute of Applied Physics) for using the ATR Spectrometer. This work has been financially supported by the Austrian Science Foundation “FWF” within the National Research Network NFN on Organic Devices (S09712-N08, S097-6000, and S9711-N08).

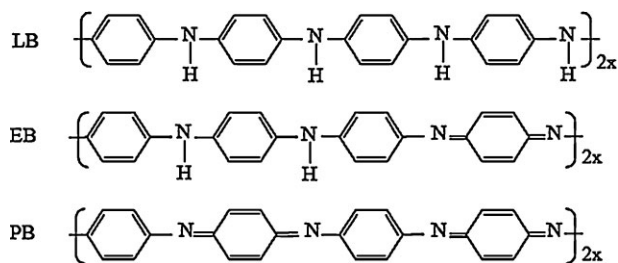


Figure 1. Fully reduced (leucoemeraldine base), half oxidized (emeraldine base), and fully oxidized (pernigraniline base) forms of polyaniline as depicted by MacDiarmid and coworkers [7, 8].

chamber with crucibles containing emeraldine base polyaniline and C_{60} . Polyaniline (emeraldine base $M_w = 5000$) is evaporated through a mask on top of a vacuum-deposited aluminum stripe acting as gate electrode in the transistor. After deposition of polyaniline and the semiconductor C_{60} , the coated glass samples are placed on a patterned mask, defining the source and drain electrodes of the transistor element. Evaporated aluminum is used for the source and drain contacts of the transistors.

Figure 3a and b shows typical atomic force microscopy (AFM) images of the evaporated polyaniline (1.75 μm thick film) and of the C_{60} film (75 nm thick) on top of the polyaniline, respectively. The surface of the polyaniline film shows a granular morphology with a peak-to-valley ratio in the range of 25–35 nm and an average root mean square (RMS) roughness value of 10 nm. The average size of polyaniline grains is around 50 nm. The C_{60} film also shows a granular morphology with peak-to-valley and RMS values in the same range as the polyaniline film on which it was grown. However, the average grain size of the buckminsterfullerene grains is around 20 nm.

In order to verify the suitability of vapor deposition for polyaniline, the evaporated films have been examined by means of Fourier transform infrared spectroscopy (FTIR) and UV-vis spectrophotometry, respectively. Polyaniline films (150 nm thick) were evaporated on KBr pellets and on glass slides. The FTIR spectra of the precursor material and the deposited film are depicted in Figure 4a and b, respectively. The peaks are assigned in accordance with values reported elsewhere.^[10,13,14,19,32–34]

The molecular weight of the deposited material is not known. It is expected however that small molecular weight

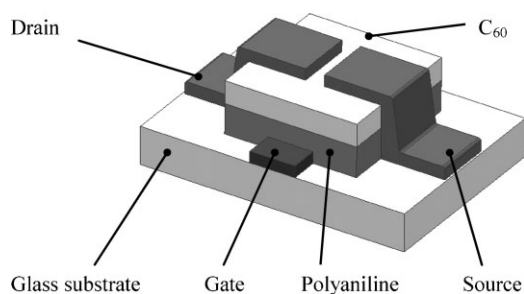


Figure 2. Scheme of the evaporation processed polyaniline- C_{60} OFET.

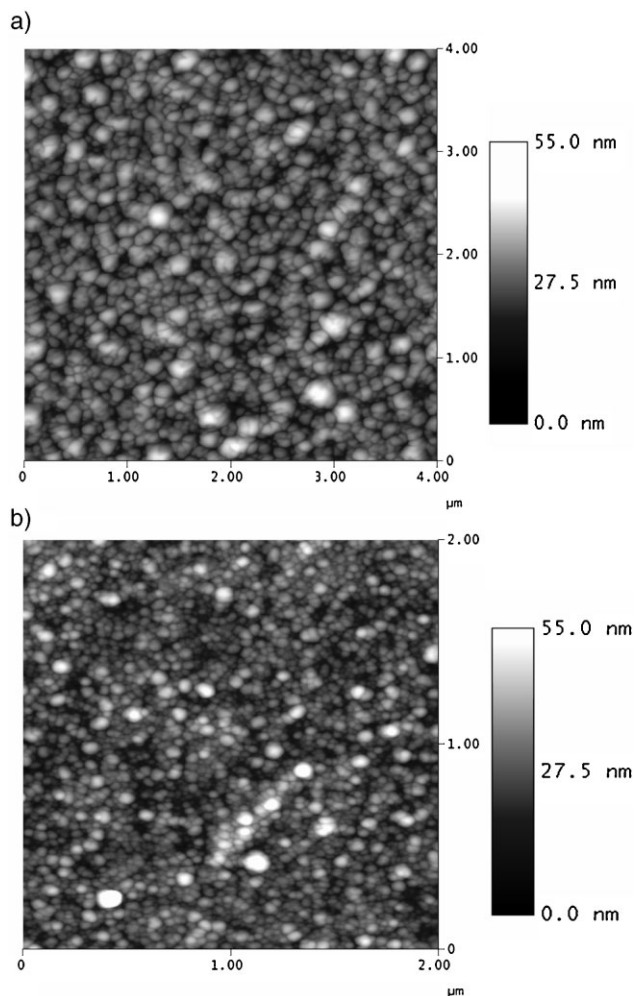


Figure 3. AFM images of the a) polyaniline surface and b) of the C_{60} surface on top of the polyaniline film.

aniline oligomers evaporate from the precursor material, condense and presumably coalesce and grow on the glass substrate. It is interesting nevertheless to observe that the vacuum deposited material is not in the same oxidation state as the precursor material, apparently due to both reduction and cross-linking processes occurring during evaporation and film growth. Chen and Lee^[32] observed a chemical cross-linking process in polyaniline thin films at temperatures in the range between 150 and 300 $^{\circ}\text{C}$, and argued that the process is responsible for the diminishing in the intensity of the peak centered at $\sim 165 \text{ cm}^{-1}$ attributed to the quinoid to diimine nitrogen stretching type vibration. Moreover, the spectrum of precursor material in the emeraldine base oxidation state displays two bands associated with N-H stretching vibrations: a band centered at $\sim 3292 \text{ cm}^{-1}$ associated with hydrogen bonded N-H stretching vibrations and another one centered at $\sim 3385 \text{ cm}^{-1}$ associated with nonhydrogen bonded free N-H type stretching vibrations. These two values are in good agreement with the published values of ~ 3290 and $\sim 3383 \text{ cm}^{-1}$, respectively, exemplified in Table 1. In contrast,

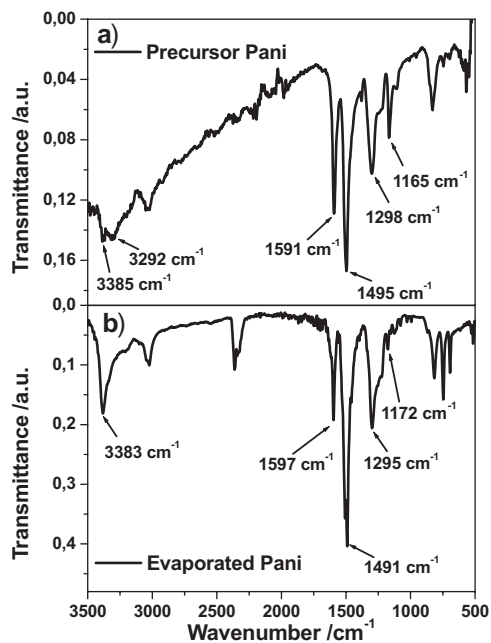


Figure 4. FTIR spectra of a) precursor polyaniline and b) evaporated polyaniline; labeled peaks correspond well with literature data summarized in Table 1.

the spectrum of evaporated polyaniline depicted in Figure 4b contains just the band centered at $\sim 3383\text{ cm}^{-1}$, which is characteristic to free, nonhydrogen bonded N–H stretching vibrations.^[14,19,32–34] In addition, the deposited sample displays a much reduced intensity in quinoid type vibrations at $\sim 1597\text{ cm}^{-1}$, however intermediate between the intensity of the peaks reported elsewhere for pure leucoemeraldine and emeraldine base oxidation states. The chemical reduction occurring in the evaporated film is confirmed also by UV–vis spectrophotometry spectra of the material before and after deposition as shown in Figure 5a and b. The characteristic peaks at ~ 330 and $\sim 628\text{ nm}$ correspond to those reported in the literature.^[5,15,18,19,32,35] In the UV–vis spectrum of the sublimated material, displayed in Figure 5b, the exciton-type absorption of the quinoid ring peak centered at $\sim 628\text{ nm}$ is not present, confirming the chemical reduction of the deposited material.

Both investigation techniques therefore indicate that the vacuum deposited material is not identical with the precursor polyaniline in the emeraldine base oxidation state, but is

Table 1. Literature assigned peaks of polyaniline infrared transmission spectra.

Peaks [cm^{-1}]	Assignment	References
~ 3383	Free N–H stretching	[14,19,32–34]
~ 3290	Interchain H bonded N–H stretching	[14,19,32–34]
~ 1590	C=C stretching-quinoid rings	[10,13,14,19,32–34]
~ 1495	C=C stretching-benzenoid rings	[10,13,14,19,32–34]
~ 1295	C–N stretching-aromatic amine	[10,13,14,19,32–34]
~ 1165	N=Q=N stretching	[10,13,14,19,32–34]

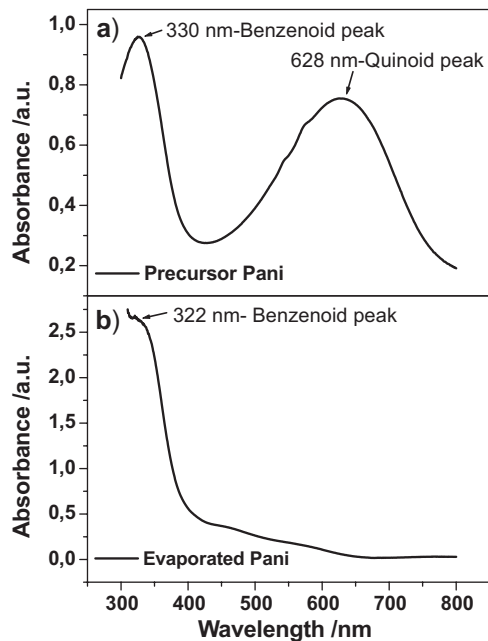


Figure 5. a) UV–vis spectra of precursor polyaniline (emeraldine base) and b) vacuum-deposited thin film (b).

actually a material with the oxidation state intermediate between the half oxidized emeraldine base and fully reduced leucoemeraldine base. This finding is in accordance with the electronic properties of polyaniline reported by other groups.^[10,29b] Nonetheless, the exact oxidation state of the deposited film is not known since during the FTIR and UV–vis investigations some oxidation of the thin films exposed to oxygen in the laboratory atmosphere could have occurred as well.

The dielectric properties of ($1.75\text{ }\mu\text{m}$ thick) evaporated polyaniline film were investigated versus applied bias voltage in the range of -15 to 15 V , and versus frequency between 20 Hz and 10 kHz , in a metal–insulator–metal (MIM) structure with 60 nm thick evaporated aluminum electrodes. The dielectric response is independent on the bias voltage and practically dispersion free in the measured frequency range. The dielectric loss angle spans between 0.02 and 0.002 in the range investigated, showing that the polyaniline film can be viewed as an insulating material. Therefore, the characterization of the highest occupied and lowest unoccupied electron energy levels is omitted for assessing the properties of polyaniline as insulator. From the measurements at 1 kHz , a dielectric constant of 3.35 with a loss tangent of 0.0045 was obtained for the evaporated polyaniline film. In order to measure the DC conductivity of the evaporated polyaniline film, the same sample used for the dielectric investigation was measured with a Keithley 617 electrometer. The measured D.C. conductivity of the polyaniline film was found to be below $5 \times 10^{-10}\text{ S cm}^{-1}$, very close to similar values reported elsewhere for hepta-aniline (LB) oligomer of polyaniline^[16] or thin evaporated polyaniline films.^[28] Therefore, both the A.C. and

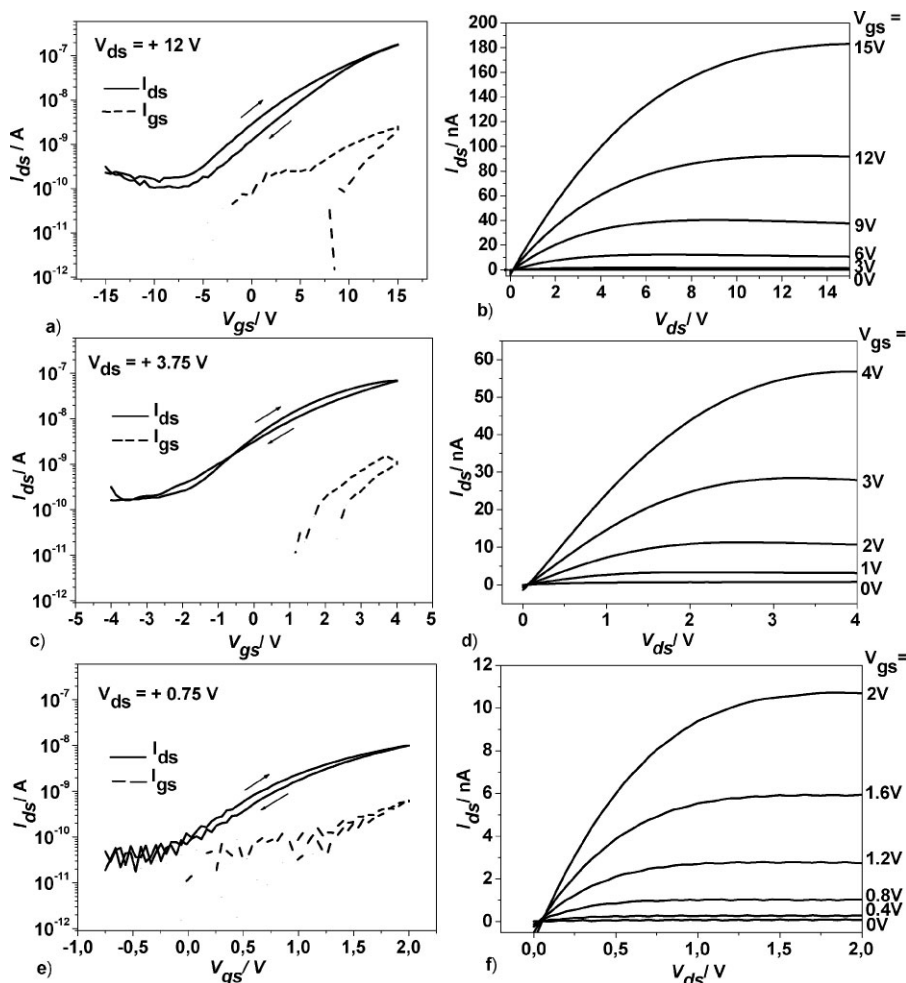


Figure 6. Transfer and output characteristics of transistors featuring 1.75 μm polyaniline and 75 nm C_{60} ; all the aluminum electrodes are 60 nm thick (a,b). Transfer and output characteristics of transistors featuring 650 nm polyaniline and 75 nm C_{60} ; the top and bottom aluminum electrodes are 60 nm thick (c,d). Transfer and output characteristics of transistors displaying 100 nm polyaniline and 25 nm C_{60} ; the top and bottom aluminum electrodes are 40 and 60 nm thick respectively (e,f).

D.C. investigations of the dielectric material suggest its suitability as gate dielectric in OFETs.

Figure 6a–f shows the transfer and output characteristics of transistors with different thicknesses of the insulator and semiconductor materials. Figure 6a–d displays transistor characteristics of devices featuring 75 nm C_{60} deposited on top of 1.75 μm and 650 nm polyaniline, respectively. Figure 6e and f displays the transfer and output curves for a “scaled down transistor” with only 100 nm polyaniline and 25 nm C_{60} thicknesses. As shown, it is possible to control the transistor characteristics by a simple variation of the insulator and/or semiconductor layer(s). We observed that for thicknesses of the insulating material in the range of 100 nm to 1.75 μm the transistors offer a change in the source to drain current in excess of three orders of magnitude and leakage currents between two to three orders of magnitude lower. The calculated electron mobility in the saturation regime, for typical transistors like the ones depicted in Figure 6a–f is

between 0.15 and 0.55 $\text{cm}^2 \text{V}^{-1} \text{s}^{-1}$, averaged over the samples fabricated under the same experimental conditions. The method employed in the mobility calculations was reported elsewhere.^[36] The electron mobility (μ) was extracted from the equation:

$$I_{D,\text{sat}} = \frac{W}{2L} C_{\text{ox}} \mu_{\text{sat}} (V_G - V_T)^2$$

where W and L represent the channel width and length respectively, C_{ox} is the insulator capacitance per unit area, and V_G and V_T are the gate and threshold gate voltages. The threshold voltage is obtained as the abscissa intercept of the line drawn through the linear part of the $I_{D,\text{sat}}^{1/2}$ versus V_G graph. In all our measured devices, the threshold voltage is positive, spanning from 0.2 to 4 V.

Both electron mobilities and transistor characteristics correlate with values already reported for C_{60} based OFETs.^[37–39] The calculated mobilities as well as the transistor characteristics were obtained on films displaying a considerable roughness (peak-to-valley ratio in the range of 25–35 nm and RMS values in the range of 8–12 nm). Working transistors featuring the above-mentioned characteristics, in the terms of on/off ratio, leakage, and electron mobilities were produced also with devices displaying a 3- μm thick dielectric with

a peak-to-valley ratio in the range of 40–60 nm, but the operating voltage reached 30 V in the latter case. On the other side of the scale, surprisingly, the thickness of pin-hole free polyaniline film could be reduced to as low as 100 nm, while still offering about a 2.5 orders of magnitude $I_{\text{on}}/I_{\text{off}}$ ratio and a leakage in the range of 1.5 orders of magnitude below the source drain current. Moreover, the operating voltage of the scaled-down transistor was as low as 2 V. The transistors display minimal clockwise hysteresis, which can be attributed to surface traps, in accordance to the polyaniline roughness revealed by the AFM images and to similar reports in the literature dealing with hysteresis effects in organic materials.^[40] The nonideal interface between the dielectric (polyaniline) and semiconductor (C_{60}) may be in fact responsible for a slow transistor characteristics (i.e., a large subthreshold swing and a consequent modest on/off ratio) as well as for a late opening (i.e., positive V_T), since it is expected that electric charges get trapped in the valleys where the potential energy is

the lowest. Various batches were produced featuring either indium-tin oxide (ITO) or Cr/Au as gate materials and Al for the source and drain electrodes, and the transistor characteristics were similar to the ones produced with Al gate. However, despite persistent effort, not a single transistor featuring Cu as gate material was working, presumably because of the high reactivity of copper toward polyaniline, observed also by Vohs and coworkers^[29d,e] The transistors from all the batches were preserved in a glove box under nitrogen atmosphere and remeasured after various periods of time, showing that the transfer and output characteristics are stable and reproducible even nine months after fabrication.

In summary, we have developed evaporation processed polyaniline and C₆₀ OFETs, with insulating polyaniline evaporated from precursor emeraldine base. The characteristics of the transistors are stable and reproducible and the fabrication method offers the versatility to adjust the operating voltage accordingly to the thickness of the deposited organic dielectric material. The ease of fabrication and the low cost of the precursor materials recommend the evaporation method as suitable for large-scale industrial production of OFETs such as R2R.

Experimental

Transistors were built on 1.5 × 1.5 cm² glass slides. Bottom gate aluminum electrodes (60 nm thick) were thermally evaporated through a patterned mask. For samples built on Cr/Au gate electrodes, the thickness of the two successively evaporated metal layers was 10 and 50 nm, respectively. The ITO gate electrodes were patterned by etching the ITO glass with “regal water”: an aqueous etching solution containing 36% hydrochloric acid, 65% nitric acid, and water in the volume ratio 0.92:0.08:1. We purchased polyaniline (emeraldine base Mw = 5000) from Aldrich, Inc. and purified it by methanol extraction until the liquid became colorless. In the final step, the material was washed copiously with deionized water (18 MΩ × cm) and dried overnight in a vacuum oven at 60 °C. It turned out that cleaning was the most important issue in the fabrication of working transistors, as also observed in solution based processing^[41]. Samples were collected from the dried powder and evaporated under a high vacuum ($p < 5 \times 10^{-6}$ bar). The C₆₀ layer was successively evaporated under the same conditions, without breaking the vacuum. To finalize the OFET devices, top aluminum electrodes with a thickness of 60 nm were thermally evaporated through a shadow mask (40 nm thick source and drain electrodes were employed for the fabrication of ultra-thin transistor). The channel length L of the OFETs is 100 μm and the channel width W is 1 mm. The overlapping electrode area of the MIM capacitor built for the dielectric measurements is 6.25 mm². The electrical characterization of all transistor and MIM devices was performed in an inert environment; the transistors were measured in a nitrogen filled glove box whereas the MIM capacitor was measured in a sample chamber under argon. For computing the electron mobility in the OFETs an experimentally measured value of capacitance per unit area ($C_{ox} = 1.63$ nF cm⁻²) was employed. An Agilent E5273A instrument was employed for the steady state current–voltage measurements and a Novocontrol Alpha Analyzer for the dielectric spectroscopy investigation. The D.C. conductivity was measured with a Keithley 617 electrometer. For the transfer characteristics of the transistors, a sweep rate of 45 mV s⁻¹ was used. The UV–vis spectrum of the pristine polyaniline was obtained by adding two droplets of 3% emeraldine base in NMP in a cuvette filled with NMP. A Cary UV–vis

spectrophotometer was used to complete the UV–vis measurements. The FTIR measurements were performed on a BRUKER OPTICS (EQUINOX 55) attenuated total reflection spectrometer. Topographical surface investigations were performed by analyzing the AFM images of the surface of the samples obtained from a Digital Instruments Dimension 3100 microscope working in tapping mode. Thickness measurements were performed with a DekTak profilometer.

Received: April 14, 2008

Revised: May 24, 2008

Published online: September 9, 2008

- [1] C. D. Dimitrakopoulos, P. R. L. Malenfant, *Adv. Mater.* **2002**, *14*, 99.
- [2] T. Anthopoulos, B. Singh, N. Marjanovic, N. S. Sariciftci, A. Ramil, H. Sitter, M. Cölle, D. de Leeuw, *Appl. Phys. Lett.* **2006**, *89*, 213504.
- [3] M. Zirkl, A. Haase, A. Fian, H. Schön, C. Sommer, G. Jakopic, G. Leising, B. Stadlober, I. Graz, N. Gaar, R. Schwödauer, S. Bauer-Gogonea, S. Bauer, *Adv. Mater.* **2007**, *19*, 2241.
- [4] A. G. MacDiarmid, J. C. Chiang, A. F. Richter, A. J. Epstein, *Synth. Met.* **1987**, *18*, 285.
- [5] J. G. Masters, Y. Sun, A. G. MacDiarmid, *Synth. Met.* **1991**, *41–43*, 715.
- [6] F. F. Runge, *Poggendorfs Ann. Phys. Chem.* **1834**, *31*, 513.
- [7] J. C. Chiang, A. G. MacDiarmid, *Synth. Met.* **1986**, *13*, 193.
- [8] W. S. Huang, B. H. Humphrey, A. G. MacDiarmid, *J. Chem. Soc. Faraday Trans 1*, **1986**, *82*, 2385.
- [9] W. S. Huang, A. G. MacDiarmid, *Polymer* **1993**, *34*, 1833.
- [10] M. Angelopoulos, G. E. Asturias, S. P. Ermer, A. Ray, E. M. Scherr, A. G. MacDiarmid, *Mol. Cryst. Liq. Cryst.* **1988**, *160*, 151.
- [11] A. J. Heeger, *Rev. Mod. Phys.* **1989**, *60*, 781.
- [12] J. Stejskal, R. G. Gilbert, *Pure Appl. Chem.* **2002**, *74*, 857.
- [13] Y. Wei, K. F. Hsueh, G. W. Jang, *Macromolecules* **1994**, *27*, 518.
- [14] W. Zheng, M. Angelopoulos, A. J. Epstein, A. G. MacDiarmid, *Macromolecules* **1997**, *30*, 2953.
- [15] X.-R. Zeng, T.-M. Ko, *Polymer* **1998**, *39*, 1187.
- [16] M. H. Lee, G. Speyer, O. F. Sankey, *J. Phys.: Condens. Matter* **2007**, *19*, 215204.
- [17] J. Libert, J. Cornil, D. A. dos Santos, J. L. Bredas, *Phys. Rev. B* **1997**, *56*, 8638.
- [18] J. Y. Shimano, A. G. MacDiarmid, *Synth. Met.* **2001**, *123*, 251.
- [19] a) M. Irimia-Vladu, J. W. Fergus, *Synth. Met.* **2006**, *156*, 1401. b) M. Irimia-Vladu, J. W. Fergus, *Synth. Met.* **2006**, *156*, 1396.
- [20] H. L. Wang, A. G. MacDiarmid, Y. Z. Wang, D. D. Gebler, A. J. Epstein, *Synth. Met.* **1996**, *78*, 33.
- [21] R. W. T. Higgins, N. A. Zaidi, A. P. Monkman, *Adv. Funct. Mater.* **2001**, *11*, 407.
- [22] F. Yakuphanoglu, B. F. Senkal, *J. Phys. Chem.* **2007**, *111*, 1840.
- [23] Y. Cao, G. M. Treacy, P. Smith, A. J. Heeger, *Appl. Phys. Lett.* **1992**, *60*, 2711.
- [24] a) K. S. Lee, G. B. Blanchet, F. Gao, Y.-L. Loo, *Appl. Phys. Lett.* **2005**, *86*, 074102. b) K. S. Lee, T. J. Smith, K. C. Dickey, J. E. Yoo, K. J. Stevenson, Y.-L. Loo, *Adv. Funct. Mater.* **2006**, *16*, 2409.
- [25] N. J. Pinto, A. T. Johnson, Jr, A. G. MacDiarmid, C. H. Mueller, N. Theofylaktos, D. C. Robinson, F. A. Miranda, *Appl. Phys. Lett.* **2003**, *83*, 4244.
- [26] Y.-C. Li, Y.-J. Lin, H.-J. Yeh, T.-C. Wen, L.-M. Huang, Y.-K. Chen, Y.-H. Wang, *Appl. Phys. Lett.* **2008**, *92*, 093508.
- [27] A. Calderone, R. Lazzaroni, J. L. Bredas, *Phys. Rev. B* **1994**, *49*, 14418.
- [28] T. R. Dillingham, D. M. Cornelison, E. Bullock, *J. Vac. Sci. Technol. A* **1994**, *12*, 2436.
- [29] a) R. V. Plank, Y. Wei, N. J. DiNardo, J. M. Vohs, *Chem. Phys. Lett.* **1996**, *263*, 33. b) R. V. Plank, N. J. DiNardo, J. M. Vohs, *J. Vac. Sci.*

- Technol. A* **1997**, *15*, 538. c) R. V. Plank, N. J. DiNardo, J. M. Vohs, *Synth. Met.* **1997**, *89*, 1. d) R. V. Plank, N. J. DiNardo, J. M. Vohs, *Phys. Rev. B* **1997**, *55*, R10241. e) K. K. Lee, J. M. Vohs, N. J. DiNardo, *Surf. Sci. Lett.* **1999**, *420*, L115.
- [30] B. Xu, A. N. Caruso, P. A. Dowben, *Appl. Phys. A* **2003**, *77*, 155.
- [31] R. F. Bianchi, H. N. da Cunha, R. M. Faria, G. F. leal Ferreira, J. Mariz, G. Neto, *J. Phys. D: Appl. Phys.* **2005**, *38*, 1437.
- [32] S.-A. Chen, H.-T. Lee, *Macromolecules* **1993**, *26*, 3254.
- [33] J. Tang, X. Jing, B. Wang, F. Wang, *Synth. Met.* **1988**, *24*, 231.
- [34] M. Angelopoulos, R. Dipietro, W. G. Zheng, A. G. MacDiarmid, *Synth. Met.* **1997**, *84*, 35.
- [35] Y. M. Lee, J. H. Kim, J. S. Kang, S. Y. Ha, *Macromolecules* **2000**, *33*, 7431.
- [36] C. R. Newman, C. Daniel Frisbie, D. A. da Silva Filho, J.-L. Bredas, P. C. Ewbank, K. R. Mann, *Chem. Mater.* **2004**, *16*, 4436.
- [37] R. C. Haddon, A. S. Perel, R. C. Morris, T. T. M. Palstra, A. F. Hebard, *Appl. Phys. Lett.* **1995**, *67*, 121.
- [38] S. Kobayashi, T. Takenobu, S. Mori, A. Fujiwara, Y. Iwasa, *Appl. Phys. Lett.* **2003**, *82*, 4581.
- [39] Th. B. Singh, N. Marjanovic, G. J. Matt, S. Gunes, N. S. Sariciftci, A. Montaigne Ramil, A. Andreev, H. Sitter, R. Schwödiauer, S. Bauer, *Org. Electron.* **2005**, *6*, 105.
- [40] J. Lancaster, D. M. Taylor, P. Sayers, H. L. Gomes, *Appl. Phys. Lett.* **2007**, *90*, 103513.
- [41] M. Egginger, M. Irimia-Vladu, R. Schwödiauer, A. Tanda, I. Frischauf, S. Bauer, N. S. Sariciftci, *Adv. Mater.* **2008**, *20*, 1018.